Deep-sea Research Part I-oceanographic Research Papers
September 2020, Volume 163 Pages 103347 (12p.)
https://doi.org/10.1016/j.dsr.2020.103347
https://archimer.ifremer.fr/doc/00643/75474/

Matching zooplankton abundance and environment in the South Indian Ocean and Southern Ocean

Godet Claire [1], Robuchon Marine [1, 2, 3, *], Leroy Boris [1], Cotté Cedric [4], Baudena Alberto [4, 5], Da Silva Ophélie [5, 6], Fabri-Ruiz Salomé [5], Lo Monaco Claire [4], Sergi Sara [4], Koubbi Philippe [7, 8]

[1] Laboratoire de Biologie des Organismes et écosystèmes Aquatiques (BOREA), Muséum National d'Histoire Naturelle, CNRS, IRD, Sorbonne Université, Université de Caen Normandie, Université des Antilles, CP 26, 57 Rue Cuvier, 75005, Paris, France
[2] Centre d'Ecologie et des Sciences de la Conservation (CESCO), Muséum National d'Histoire Naturelle, CNRS, Sorbonne Université, CP 135, 57 Rue Cuvier, 75005, Paris, France
[3] Joint Research Centre (JRC) of the European Commission, Directorate for Sustainable Resources, Ispra, Italy
[4] Sorbonne Université UMR 7159 CNRS-IRD-MNHN, LOCEAN-IPSL, 75005, Paris, France
[5] Laboratoire D'Océanographie de Villefranche-sur-Mer, UMR 7093 - CNRS/UPMC, 181 Chemin Du Lazaret, 06230, Villefranche-sur-Mer Cedex, France
[6] Institut de Systématique, Evolution, Biodiversité (ISYEB), Muséum National d'Histoire Naturelle, CNRS, Sorbonne Université, EPHE, Université des Antilles, CP 50, 57 Rue Cuvier, 75005, Paris, France
[7] UFR918 Terre, Environnement, Biodiversité. Sorbonne Université, 4 Place Jussieu, 75252, PARIS Cedex 05, France
[8] IFREMER Centre Manche Mer Du Nord - 150, Quai Gambetta, 62200, Boulogne-sur-Mer, France

* Corresponding author : Marine Robuchon, email address : marine.robuchon@ec.europa.eu

Abstract :

Distinguishing regions based on the geographic distribution of both abiotic factors and living organisms is an old but still actual central issue for biogeographers. In the Southern Ocean, the few existing regionalization studies have been carried out either at very large scales or on the relatively small region around the Sub-Antarctic islands of Kerguelen and the Crozet archipelagos. However, regionalization studies at meso-scales (100–300 km) covering the Indian part of the Southern Ocean and adjacent South Indian Ocean are scarce. These waters, ranging from the Subtropical to the polar region, are home to large populations of well-studied top predators that depend on the biomass of less known mid-trophic level species such as zooplankton. To fill those gaps, our study aims at conducting bioregional analyses of this transition area at the meso-scale based on the distribution of abiotic factors and chlorophyll-a, and to investigate how the abundance of zooplankton varies across the bioregions identified. To that end, we first characterized epipelagic bioregions 30°S in the South Indian Ocean to 65°S in the Southern Ocean and from 40° to 85°E including the islands of Crozet, Kerguelen, Saint-Paul and New Amsterdam. We then determined whether these bioregions correspond to variations in the abundance of zooplankton collected by a Continuous Plankton Recorder. Finally, we analyzed which environmental parameters influence zooplankton abundance. Our analyses evidenced six regions, providing a synthetic overview of

a contrasting environment. The spatial variability of zooplankton abundance was explained by most of the environmental variables used in the bioregionalisation and, to a lesser extent, by the bioregions. Copepods are abundant in the colder and physically-energetic regions associated with the Antarctic Circumpolar Current (ACC). Limacina and euphausids are both abundant in regions characterized by a high concentration of chlorophyll-a, although euphausids are also abundant in the subtropical region. This work represents a crucial step forward in the integration of living organism distribution in the regionalization of the Indian part of Southern Ocean and adjacent South Indian Ocean. This can, ultimately contribute to the optimization of marine conservation strategies.

Highlights

► Bioregionalization studies at mesoscale in the Southern/Indian Oceans are scarce. ► We delineated 6 pelagic bioregions in this area from environmental parameters. ► These bioregions are: the Shelf and high productivity off-shelf waters, the deep Eastern Part of the Enderby basin, the High turbulence areas of the Sub-Antarctic and Subtropical fronts, the Island shelves less productive areas and seamounts, the Indian Ocean Deep and the Indian ridges subtropical. ► Environmental parameters better explain variations in zooplankton abundance than bioregions.

Keywords : Bioregionalization, Southern Ocean, Indian Ocean, Pelagic ecosystem, Zooplankton, Continuous plankton recorder

1. INTRODUCTION

Marine ecoregionalization is a process that aims to divide oceanic areas into distinct spatial regions, using a range of abiotic and biotic – such as chlorophyll-*a* and species assemblages – information (Foster et al, 2017; Hill et al, 2017; Koubbi et al, 2010; Koubbi et al., 2011; Spalding et al., 2007). When data on species assemblages are not sufficiently available to identify ecoregions accurately, bioregions (Grant et al., 2006) or biogeochemical regions (Longhurst, 2010) can be identified based on the distribution of abiotic factors and chlorophyll-*a* only, i.e. available satellite gridded products. The process results in a set of bioregions, each with relatively homogeneous and predictable ecosystem properties (Grant et al., 2006). Bioregions can be divided at different spatial scales, depending on their physical and environmental characteristics. Bioregions are considered as a proxy of biodiversity spatial patterns through an objective zoning. They constitute a basis for understanding, conserving and managing activities in the marine environment (Grant et al., 2006; Ainley et al., 2010; Hogg et al., 2018).

Several studies have proposed regionalizations based on the biogeochemical, hydrological or physical and geographical characteristics of the oceans including the Southern Ocean (Grant et al., 2006; Longhurst, 2010; Raymond, 2014; Reygondeau et al., 2014). Four biogeochemical provinces have been identified in the Southern Ocean (Longhurst, 2010) from publications on satellite observations, oceanographic and biotic observations on chlorophyll-*a*, phytoplankton or zooplankton collected during oceanographic surveys. Major changes in these biogeochemical provinces are projected by modeling studies, including southward shifts of the provinces and changes in their areas (Reygondeau et al., 2014). Changes in the Southern Ocean are mainly imputed to the consequences of human activities, both direct (exploitation of living resources by fishing) and indirect (increase in temperature, seasonality of sea ice, ocean acidification; Constable et al., 2014; Turner et al., 2014; IPCC, 2019). These alter the functioning of marine systems and food webs because they induce habitat

modifications, which affect primary producers up to top predators, coastal organisms down to deep species, and the Sub-Antarctic Zone up to the sea ice zone (Constable et al., 2014; Gutt et al, 2015).

However, the existing Southern Ocean regionalizations (Grant et al., 2006; Raymond, 2014) did not consider regional features such as phytoplankton plumes linked to island effects and did not include seasonality. In addition, their northern limit (40°S) excluded the Subtropical zone. This paper proposes to delimit bioregions for the South Indian Ocean and the Southern Ocean covering the area between 40°E and 85°E; 30°S and 65°S. These include the islands of Crozet, Kerguelen, Saint Paul and New Amsterdam. These islands are linked to important topographic features, the ridges of southwest and southeast Indian Del Cano elevation, Crozet Islands' shelf (archipelago) and the Kerguelen Plateau. The occurrence of different water masses and the interaction of the intense ACC with these bathymetric features contribute to the heterogeneity of the region, both from an hydrodynamical point of view and for the subsequent distribution of biogeochemical properties (Roquet et al., 2009; Sokolov and Rintoul, 2007). In this area, the large-scale distribution of primary production and top predators are well known, respectively from remote sensing and biologging data (Cotté et al., 2007; Bost et al., 2009; De Monte et al., 2012; Gandhi et al., 2012; Ropert Coudert et al., 2014). However, very few studies have examined the regional distribution of zooplankton and intermediate trophic levels such as micronekton which includes small organisms (~1–20 cm or g) that can swim (Koubbi, 1993; Handegard et al., 2013; Duhamel et al., 2014; Lehodey et al., 2015; Behagle et al., 2016; Venkataramana et al., 2019). In addition, the main studies on plankton have been mostly conducted in around Kerguelen, either in the coastal zone, above the island shelf or on the eastern edge of the plateau (Blain et al., 2007; Pollard et al., 2007; Sanial et al., 2014).

Sampling devices gathering large scale zooplankton information, like the Continuous Plankton Recorder (CPR), can survey vast geographical region to study zooplankton

distribution (Batten et al., 2019). This plankton sampling device continuously collects organisms all along a cruise track at the sub-surface and has already been deployed in the Southern Ocean for past studies (Hosie et al., 2003 and 2014). The CPR was deployed for the first time in the South Indian Ocean and the Southern Ocean in 2013 on board the R/V "Marion Dufresne" (Meilland et al., 2016) and since then the surveys have been carried out every year between January and February (Fig. 1). These new samples at high spatial resolution fill a geographic gap in both the South Indian Ocean and the Southern Ocean.

Therefore, the objectives of this study were (i) to delimit and characterize bioregions in this area and (ii) to verify whether variations in the abundance of zooplankton can be explained by the environmental characteristics of the bioregions. Specifically, we wanted to define these bioregions at the mesoscale (100-300 km) to provide a better representation of oceanographic features, such as water mass dynamics and fronts. To attain our general objectives, we first delimited summer pelagic bioregions on the basis of environmental parameters (sea surface temperature, chlorophyll-*a* concentration, kinetic energy and bathymetry) describing the main characteristics of the region analyzed. Then, we determined whether these bioregions were precise predictors of variations in zooplankton abundance in the Southern Ocean and the South Indian Ocean by using samples collected by the CPR. Finally, we investigated the extent to which changes in zooplankton abundance were explained by the environmental characteristics of bioregions.

2. MATERIALS AND METHODS

2.1. Bioregionalization

2.1.1. Study area

Our study area lies between 40°E and 85°E; 30°S and 65°S (Fig. 1) and includes large latitudinal gradients in water masses proprieties with different fronts separating the subtropical waters from the polar waters (Orsi et al., 1995). These fronts are associated with the ACC which is very intense in this area. Some of these fronts depict drastic changes in temperature and salinity (Post et al., 2014; Park et al., 1991 and 1993) and delimit large oceanographic regions. The Subtropical Front (STF) defines the southern limit of warm and oligotrophic waters that characterize the subtropical gyre. Further south lies the Sub-Antarctic Front (SAF) associated to the main core of the ACC (Park et al., 2002, 2008), followed by the Antarctic Polar Front (PF). The Sub-Antarctic Zone extends between the STF and the SAF, while the Polar Frontal Zone extends between the SAF and the PF. The Subtropical Zone is located to the north of the STF. In this area, the Sub-Antarctic Zone corresponds to a narrow band of about 2° of latitude (between 44°S and 46°S) that is formed by the convergence of the SAF and STF, in the East of the Kerguelen shelf the PF is also close to the other fronts (Park et al., 1991 and 1993). The largest extent of the Polar Frontal Zone is found to the south of Crozet (between 45°S and 52°S), while it covers only a few degrees in latitude to the north-east of Kerguelen (Sokolov and Rintoul, 2009). The Subtropical Zone also includes the Agulhas Return Current, current which influences species assemblages in the western subtropical part of the area (Koubbi, 1993). On a longitudinal scale, several shallow island shelves and seamounts diversify the geomorphological landscape and shape the ocean circulation. The Kerguelen plateau is a major bathymetric feature extending from the Kerguelen island shelf towards the Antarctic shelf. It deeply, influences the hydrology of the area. It acts as a barrier deflecting the ACC which flows continuously through the Southern Ocean due to the absence of continental lands (Roquet et al., 2009). The study area is also highly heterogeneous in terms of biological productivity. Most of the ice-free polar waters in the Permanent Open Ocean Zone (zone between 50° and 60°S; Pondaven et al., 1998) are characterized by High Nutrient Low Chlorophyll (HNLC; i.e. phytoplankton are not abundant

whereas there are high macronutrient levels) conditions due to iron limitation. This trace element limits the primary production in the study area (Martin, 1990; De Baar et al., 1995). The HNLC region contrasts with the intense phytoplankton blooms occurring close to iron sources, notably around the Sub-Antarctic islands. There, the iron is delivered by the interaction of the flow and the shallow topography (Boyd and Ellwood, 2010). This physical and biogeochemical process supports recurrent phytoplankton blooms, occurring during spring over the plateau between Kerguelen and Heard Islands (southeast of Kerguelen), north and east of Kerguelen (Blain et al., 2007; Park et al., 2008), as well as north and east of Crozet (Pollard et al., 2007; Sanial et al., 2014). Conversely, the upstream waters of Kerguelen and Crozet are generally less productive.

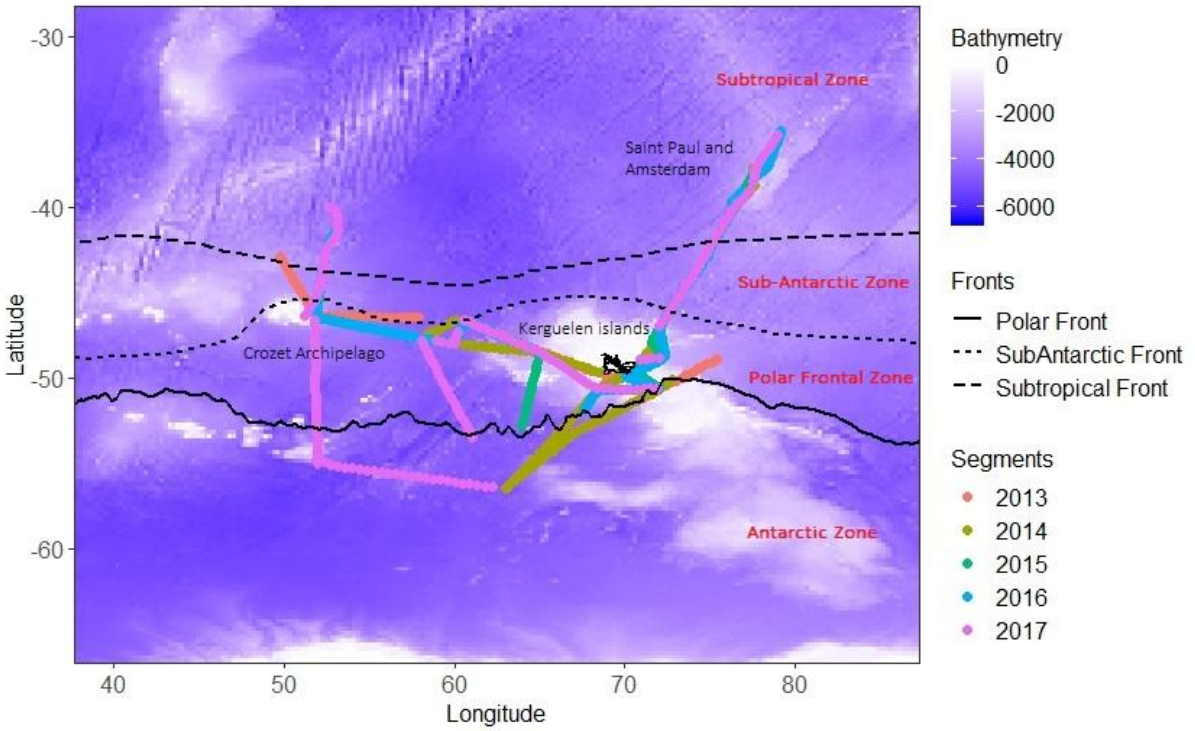

Fig. 1. Map of the study area showing the routes of the oceanographic vessel for each year (2013-2017), the different fronts of the represented area (Subtropical Front, Sub-Antarctic Front and Polar Front) and the different zones of the area (Subtropical Zone, Sub-Antarctic

169 Zone , Polar Frontal Zone and Antarctic Zone). The position of the fronts follows Park et al.
170 (2014).

171 *2.1.2. Environmental data*

172 Our first objective was to delineate bioregions on the basis of four environmental parameters:
173 (i) sea surface temperature, which varies latitudinally in the study area, (ii) chlorophyll-*a*
174 concentration, which is an indicator of phytoplankton abundance and iron enrichment zones,
175 (iii) kinetic energy, which identifies physically-energetic zones associated with the ACC and
176 (iv) bathymetry, which distinguish shelf from open ocean zones.

177 Oceanographic data were obtained from satellite measurements from 2013 to 2017 for
178 the period from November to March (i.e. during Austral summer). The parameters studied
179 were sea surface temperature (SST, in °C), chlorophyll-*a* concentration (Chl-*a*, in mg.m-3),
180 kinetic energy (KE, in $m^2.s^{-2}$) and bathymetry (Bat, in m) (Table 1). Each environmental
181 parameter had a different spatial resolution. In order to manage these differences, we carried
182 out bioregionalization at the lowest resolution of the environmental parameters, i.e. the spatial
183 resolution of the kinetic energy at 0.25°.

184 **Table 1.** Description of environmental parameters used in this study

Environmental parameters	**Abbreviations**	**Source and products**	**Spatial Resolution**	**Daily resolution**
[Chlorophyll-*a*] (mg.m-3)	Chl-*a*	Copernicus Marine Environmental Monitoring Service website (http://marine.copernicus.eu/): "OCEANCOLOUR_GLO_CHL_L4_REP_OBSERVATIONS_009_082" for 2013 and 2014 data and "OCEANCOLOUR_GLO_CHL_L4_NRT_OBSERVATIONS_009_033" (satellite products).	0.04°	8 days mean
Sea Surface	SST	Copernicus Marine Environmental Monitoring Service	0.05°	Daily

Temperature (°C)		website (http://marine.copernicus.eu/): "SST_GLO_SST_L4_NRT_OBSERVATIONS_010_001" (satellite products).		mean
Kinetic Energy ($m^2.s^{-2}$).	KE	KE data were obtained from the zonal and southern velocity (U and V, respectively) which estimate surface currents derived from altimetry through a geostrophic approximation. U and V are provided in the 'SEALEVEL_GLO_PHY_L4_REP_OBSERVATIONS_008_047' product which was downloaded from the E.U. Copernicus Marine Environment Monitoring Service (CMEMS, http://marine.copernicus.eu/ for the period 2013-2017. In this way, an estimation of the total kinetic energy is obtained.	0.25°	Daily mean
Bathymetry (m)	Bat	http://www.gebco.net (satellite products)	0.008°	/

The KE was calculated from the altimetry-based horizontal current velocities, using the following formula:

$$KE = 0.5*(U^2+V^2)/1000,$$

where U and V are the zonal (i.e. longitude) and meridional (i.e latitude) velocities. The bathymetry of the study area was downloaded from the General Bathymetric Chart of the Oceans website (www.gebco.net).

Oceanographic data were downloaded for the period November to March for the years 2013, 2014, 2015, 2016 and 2017. The raw data correspond to daily averages for the SST and KE parameters and weekly averages for the Chl-*a* parameter, due to the very high cloud cover in the study area. Data were then analyzed using the mean value calculated over the summer period (November to March).

197 *2.1.3. Zooplankton sampling and identification*

198 Zooplankton was sampled using a CPR on board the R/V “Marion Dufresne” every summer,
199 between January and February, from 2013 to 2017, for a total of 1282 samples corresponding
200 to 6410 nautical miles. The CPR is a mechanical device that allows continuous sampling of
201 plankton while being towed in the subsurface behind the vessel (at a speed from 10 to 15
202 knots). The CPR was towed approximately 100 m behind the vessel at a depth varying
203 between 10 and 30 m. The CPR works as follows: water enters through a square opening
204 (1.62 cm^2: 1.27x1.27 cm) into a collecting tunnel (10x5 cm). The plankton then reaches a
205 moving silk band (filter silk) with an average mesh size of 270 μm. A second strip of silk
206 (covering silk) covers the filtering silk and is then wound in the fixing tank, which contains
207 diluted formaldehyde. Regardless of the speed of the vessel, the silk advances at a speed of
208 about 1 cm per nautical mile during towing (Hunt and Hosie, 2003; Hosie et al., 2014).

209 In the laboratory, each set of silk is unwound and cut by segments of 5 nautical miles.
210 The entire content of each sample is identified at a coarse taxonomic resolution and assigned
211 to one of the following groups: copepods, euphausids, amphipods, *Limacina,* chaetognaths
212 and ostracods, which are counted under a stereomicroscope. For each major taxon, the
213 individuals are counted in the fraction where at least 100 individuals of that taxon are found.
214 For this a Folsom splitter was used.

215 Zooplankton abundance data obtained by the CPR (2013-2017) for each taxon and silk
216 sample and the corresponding metadata (GPS coordinates) were stored in a table. The
217 abundances were calculated (number of individuals per nautical mile) and each sample was
218 assigned to the time of day (Day, Dusk, Night, Dawn) which was calculated using the solar
219 angle ("RAtmosphere" package; Biavati, 2014). The number of samples is 552 during the day,
220 167 at dusk, 338 at night and 225 at dawn.

221 **2.2. Data processing and statistical analyses**

All statistical analyses were done using R (R Core Team, 2018) and the maps were realized using either R or using a Geographic Information System (ArcGIS v. 10.5.1.).

2.2.1. Bioregionalization

The first step in the bioregionalization procedure was to conduct a principal component analysis (PCA, Legendre and Legendre, package "FactoMineR", 1998; Lê et al., 2008) on environmental parameters (SST, KE, Bat and Chl-*a*) to eliminate noise before classification (concentration of information on the first components), resulting in a more stable classification. The second step consisted of clustering sites by applying the method of K-means (MacQueen, 1967) on the coordinates of site on the two first PCA axes. The optimal number of clusters (in this study, the environmental envelopes of bioregions) was chosen using the index of Calinski Harabasz (1974) and the elbow method (NG, 2012). The final step was to create a map of bioregions based on the clusters obtained.

2.2.2. Characterization of zooplankton sampling

To study variations in zooplankton abundance (log(abundance+1)) between the different taxa, a Kruskal-Wallis analysis was conducted. The same analysis was performed without zero values of abundance for each taxon, to take into account the fact that some taxa live in schools in the Southern Ocean. After each Kruskal-Wallis analysis, post-hoc pairwise Wilcoxon rank sum tests were carried out. This consisted of a multiple comparison test with correction by the Holm method (1979) between each pair of taxa to unravel the differences between them.

2.2.3. Analyses of variation in plankton abundance

The following analyses were carried out on the total abundance of zooplankton (including data with zero values). To investigate how zooplankton abundance (log(abundance+1)) varied according to the period of the day, a Kruskal-Wallis analysis was performed. The same analysis was performed to test differences in abundances between years. Post-hoc pairwise

Wilcoxon rank sum tests were also carried out to unravel the differences between each pair of periods of the day.

These analyses focused on copepods, euphausids and *Limacina*, which were the most abundant taxa. Night samples were used for this analysis because at night, zooplankton abundance and diversity are higher due to nocturnal migrations. A Kruskal-Wallis test was used to study variations in the abundance of copepods, euphausids and *Limacina* between the different bioregions. A Kruskal-Wallis test was used to study variations in the abundance of copepods, euphausids and *Limacina* in the different bioregions. Subsequent post-hoc pairwise Wilcoxon rank sum tests were carried out to reveal the differences between each pair of bioregions regarding the abundance of each taxon. Then, a generalized linear model (with Poisson distribution) was used to study the fluctuations in the abundance of the different taxa as a function of different environmental parameters (SST, the log of KE, the log of Chl-*a* and the log of Bat).

3. RESULTS

3.1. Characterization of bioregions

The first two axes of the PCA on environmental variables explained 70% of the total variance (Fig. 2). Axis 1 permitted to discriminate sites according to KE and SST while axis 2 permitted to discriminate sites according to Bat and Chl-*a*. The clustering on the first two axes of the PCA on environmental variables identified six distinct bioregions, a number of clusters that allowed us also to describe the study area with sufficient detail to make sense from an ecological point of view (Fig. 2). Indeed, Axis 1 opposes bioregions with relatively high KE and SST (Bioregions 3, 5 and 6) to bioregions with lower KE and SST (Bioregions 4 and 2) and axis 2 further opposes one bioregion with high Chl-*a* and Bat (Bioregion 1) to the others (Fig. 2). The 6 bioregions are mapped and their environmental variability described in Fig. 3,

while Table 2 provides a synthetic overview of their localization and environmental characteristics.

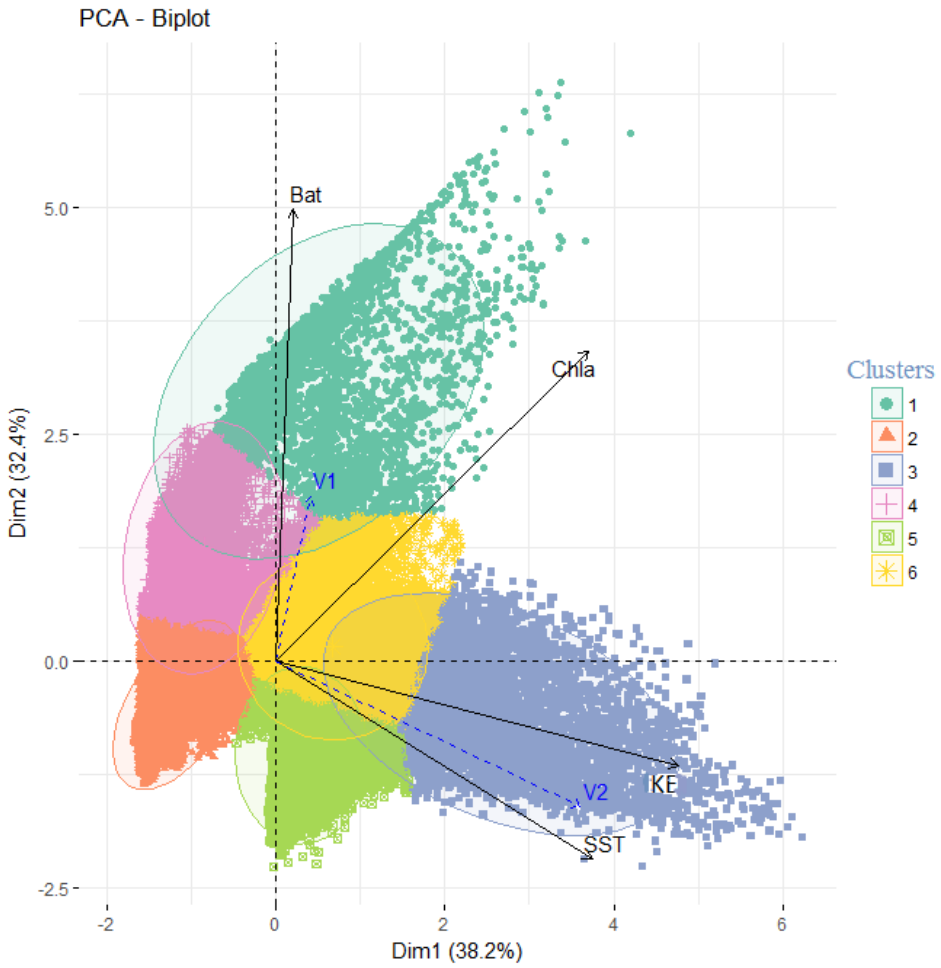

Fig. 2. Principal Component Analysis (PCA) of environmental parameters (SST: Sea Surface Temperature (°C); KE: Kinetic Energy ($m^2.s^{-2}$); Chl-*a*: concentration of Chlorophyll-*a* (mg.m-3) and Bat: Bathymetry (m)) on the two first significant axes of the PCA (Dim1, Dim2)). V1= longitude and V2= latitude are supplementary variables that do not influence the PCA. The colour of the 6 clusters is represented on the observations and concentration ellipses.

281

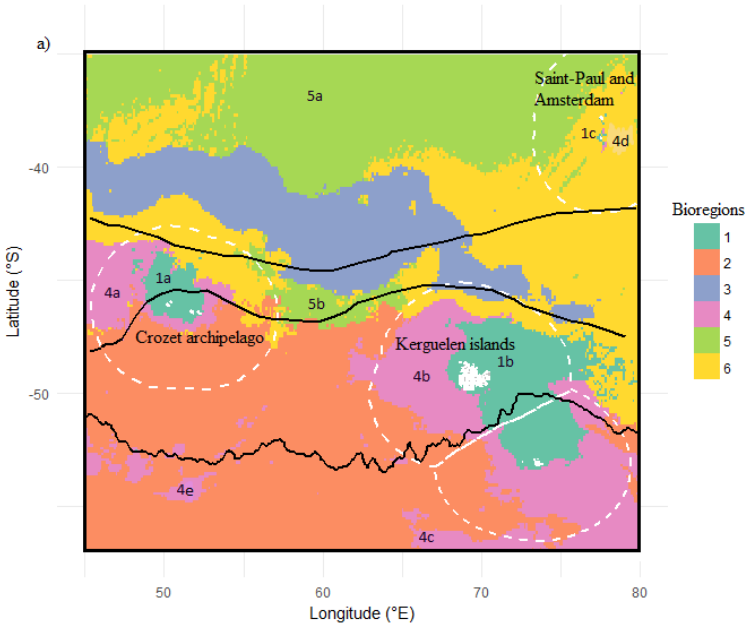

282

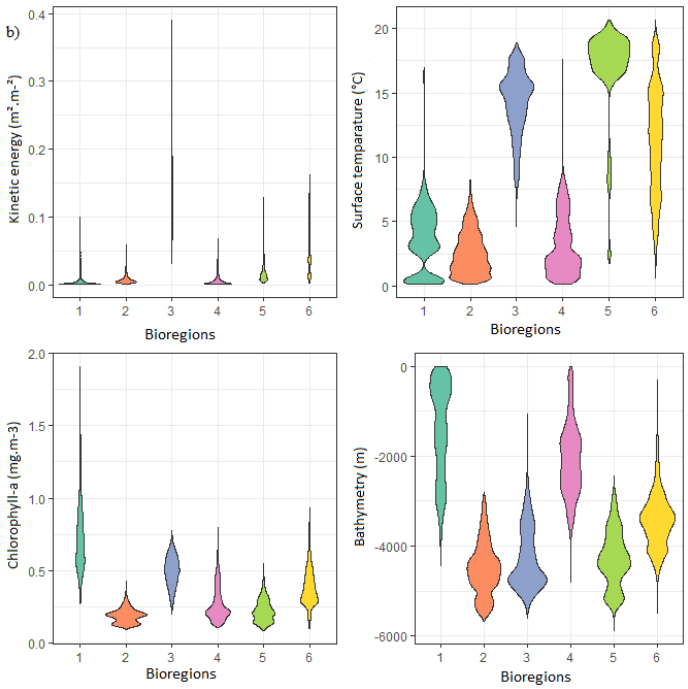

283 **Fig. 3.** Bioregions defined by SST, KE, Chl-*a* and Bat (SST: Sea Surface Temperature; KE:
284 Kinetic Energy; Chl-*a*: concentration of Chlorophyll-*a* and Bat: Bathymetry). Map of the six
285 bioregions and position of the 3 main hydrological fronts (from north to south: STF, SAF and
286 PF), the white dashed lines correspond to the exclusive economic zones (a). Violin plots of
287 environmental parameters (SST, KE, Chl-*a* and Bat) according to the six bioregions (b).

288 **Table 2.** Descriptions of the six bioregions identified in the study area and shown in Fig. 2
289 and Fig. 3.

Bioregions	Localization	Characteristics
1	Shelf and high productivity off-shelf waters	-Cold SST (min=0.11°C, mean= 3.57°C, max=16.96°C) -Low KE(min= 0.00 $m^2.s^{-2}$, mean= 0.00 $m^2.s^{-2}$, max= 0.09 $m^2.s^{-2}$) -High Chl-*a* (min=0.27 $mg.m^{-3}$, mean= 0.73 $mg.m^{-3}$, max= 1.91 $mg.m^{-3}$) - Shallow sea (min=-4443.0m, mean=-1434.7m, max=-2.0m)
2	Deep Eastern Part of the Enderby basin	-Cold SST (min=0.19°C, mean=2.59°C, max=8.21°C) -Low KE (min=0,00 $m^2.s^{-2}$, mean=0.01 $m^2.s^{-2}$, max=0.05 $m^2.s^{-2}$) -Low Chl-*a* (min=0.09 $mg.m^{-3}$, mean=0.19 $mg.m^{-3}$, max=0.42 $mg.m^{-3}$) -Deep sea (min=-5680m, mean=-4499m, max=-2801m)
3	High turbulence areas of SAF and SFT	-Hot SST (min=4.66°C, mean=14.29°C, max=18.93°C)

		-High KE (min=0.03 m².s-², mean=0.15 m².s-², max=0.39 m².s-²) -Moderate Chl-*a* (min=0.20 mg.m-3, mean=0.50 mg.m-3, max=0.77 mg.m-3) -Deep sea (min=-5595m, mean=-4271m, max=-1072m) This ecoregion is highly influenced by KE
4	Island shelves less productive areas and seamounts	-Cold SST(min=0.18°C, mean=3.16°C, max=17.62°C) -Low KE (min=0.00 m².s-², mean=0.01 m².s-², max=0.06 m².s-²) -Low Chll-*a* (min=0.10 mg.m-3, mean=0.26 mg.m-3, max=0.80 mg.m-3) -Shallow sea (min=-4791m, mean=-2087m, max=-13m)
5	Indian Ocean Deep	-High SST (min=1.74°C, mean=17.01°C, max=20.69°C) -Low KE (min=0.00 m².s-², mean=0.02 m².s-², max=0.12 m².s-²) -Low Chl-*a* (min=0.08 mg.m-3, mean=0.22 mg.m-3, max=0.55

		mg.m^{-}3) -Deep sea (min=-5887m, mean=-4283m, max=-2437m)
6	Indian ridges subtropical	-High SST (min=0.62°C, mean=7.98°C, max=20.69°C) -Low KE(min=0.00 m².s-², mean=0.05 m².s-², max=0.16 m².s-²) -Low Chl-*a* (min=0.10 mg.m^{-}3, mean=0.38 mg.m^{-}3, max=0.93 mg.m^{-}3) -Deep sea (min=-5497m, mean=-3433m, max=-319m)

290

291 **3.2. Characterization of zooplankton sampling**

292 The Kruskal-Wallis test showed that the abundance of zooplankton sampled in the surface
293 layer varied significantly between the different taxa (Fig. 4a). Specifically, we found that (i)
294 copepods were more abundant than the other taxa, (ii) the abundance of copepods was not
295 significantly different from the total abundance, (iii) *Limacina* and amphipod taxa present
296 similar abundances.

297 In addition, when performing the same analyses without the zero abundance values of
298 the different taxa, we found that the abundance of copepods, euphausids and *Limacina*
299 differed significantly from each other (Fig. 4b). As the abundance of euphausids and
300 *Limacina* was significantly higher than the abundance of ostracods, chaetognaths and

amphipods (Fig. 4b) and represent the vast majority of the zooplankton sampled, we decided to focus the following statistical analyses only on copepods, euphausids and *Limacina*.

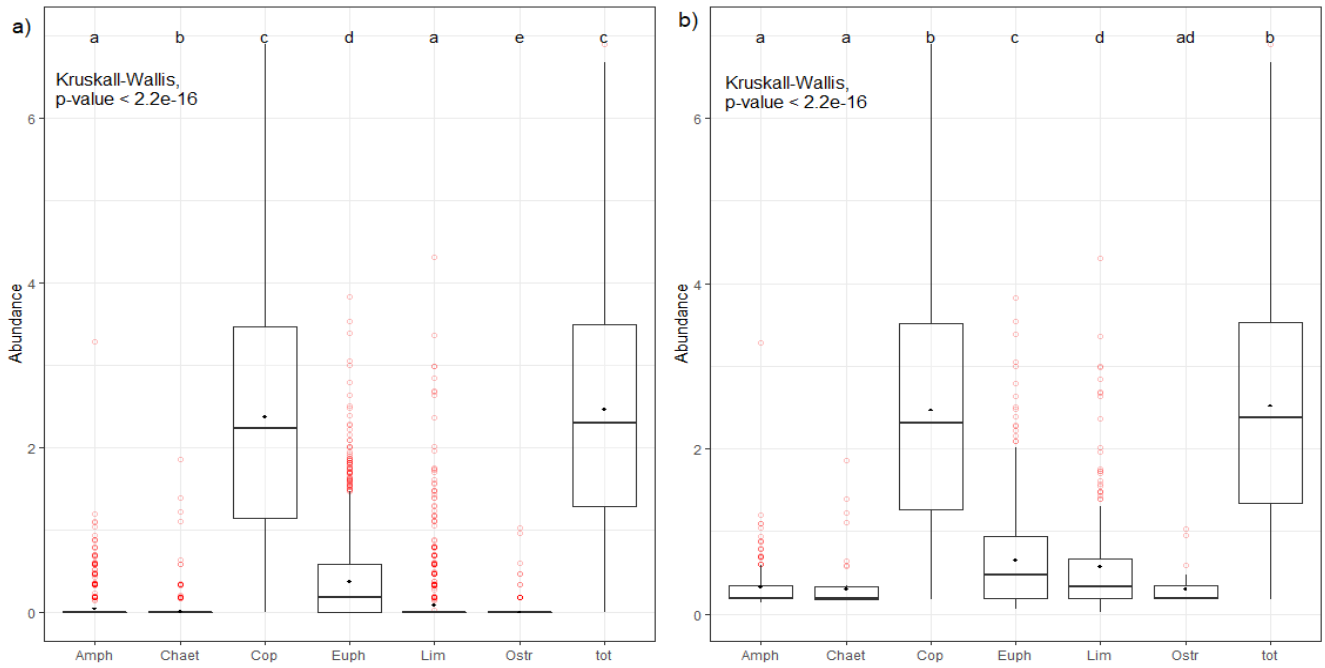

Fig. 4. Distribution of values of abundance by taxon (number of individuals per nautical mile) (Amph = Amphipods, Chaet= Chaetognaths, Cop = Copepods, Euph= Euphausiids, Lim = *Limacina*, Ostr= Ostracods, tot= total zooplankton abundance). On the left the abundance values are transformed into log(x+1) (a) and on the right the abundance values are transformed into log(x+1) and without the zero values (b). The outliers are in red. Following the Wilcoxon post-hoc tests, the letters (a, b, c, d, e) correspond to the representation of significance. If two taxa share the same letter then they are not significantly different, and on the contrary, if two taxa do not share the same letter, then they are significantly different.

3.3. Temporal variations in zooplankton abundance

Kruskal-Wallis analyses and the post-hoc tests of Wilcoxon generally showed that the abundance of zooplankton sampled in the surface layer was significantly higher at night and lower during the day (Fig. 5a). Kruskal-Wallis analyses showed that the abundance of

317 zooplankton sampled in the surface layer did not vary significantly from year to year (Fig.
318 5b).

319

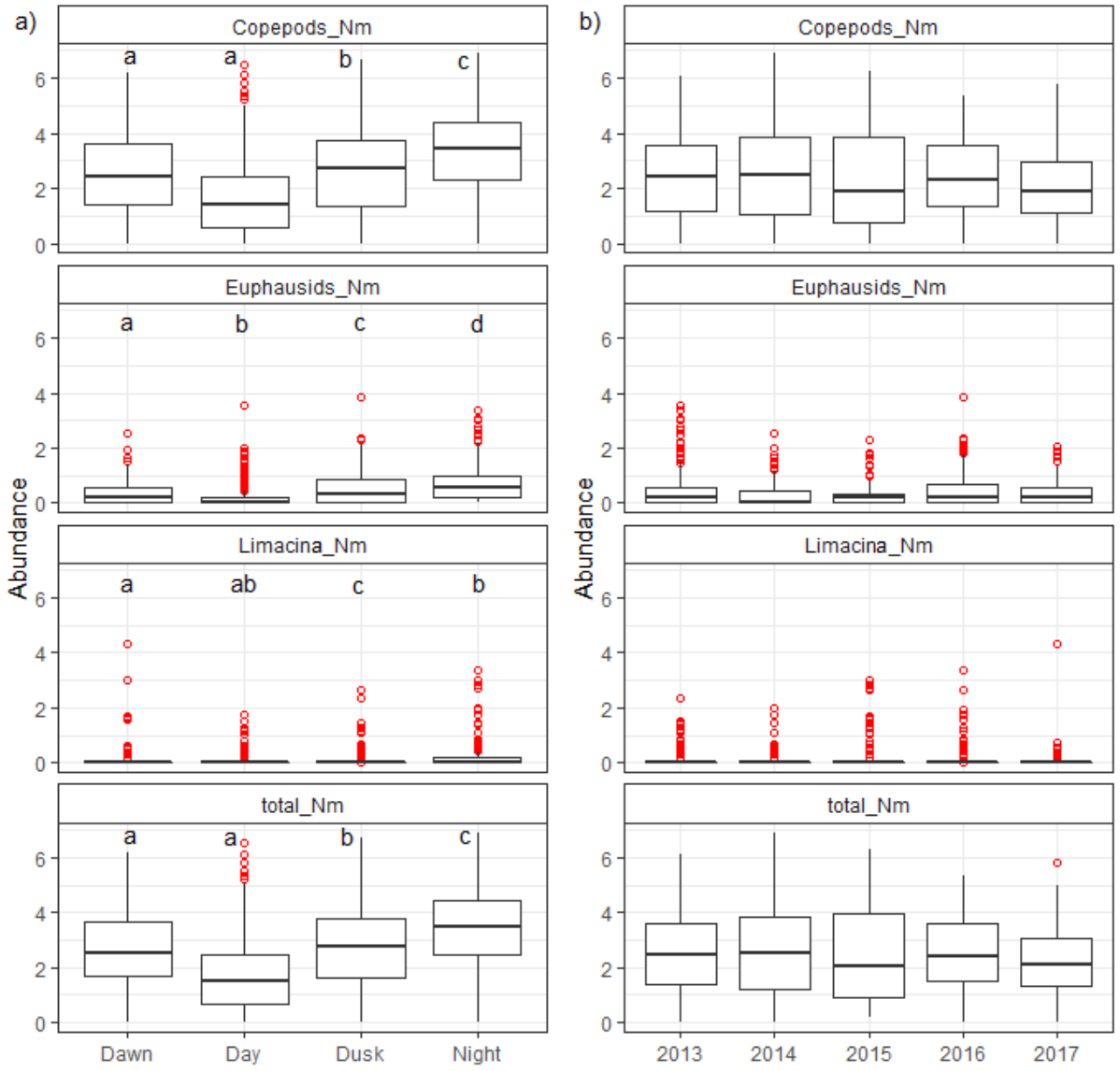

320

321 **Fig. 5.** Distribution of abundance value of copepods, euphausids, *Limacina* and total
322 abundance of zooplankton transformed into a log (x+1) (number of individuals per nautical
323 mile (Nm)) according to different periods of the day (a). Distribution of abundance values of
324 copepods, euphausids, *Limacina* and total abundance of zooplankton transformed into a log
325 (x+1) (number of individuals per nautical mile,) according to different years (b). The outliers
326 are in red. Following the Wilcoxon post-hoc tests, the letters (a, b, c, d, e) correspond to the

representation of significance. If two periods of the day share the same letter, then they are not significantly different, and, on the contrary, if two periods of the day do not share the same letter, then they are significantly different.

3.4. Variations in zooplankton abundances across bioregions

The copepod, *Limacina* and total night abundances did not differ significantly between Bioregions 1 to 5 (Fig. 6). Nonetheless, copepod, *Limacina* and total night abundances were the lowest in Bioregion 6, with significant differences with Bioregions 1, 2, and 4 depending on the group (Fig. 6). Euphausid abundance did not differ significantly among Bioregions 1 and 3 to 6, but was significantly lower in Bioregion 2 than in Bioregions 1 and 6 (Fig. 6).

The bioregions identified in the cluster analysis are differently represented by the zooplankton samples. In particular, Bioregion 3 and Bioregion 5 are largely under-sampled with respectively 3 and 11 samples collected within the five campaigns. This may explain why the zooplankton abundance found there did not differ significantly from any bioregion (Fig. 6).

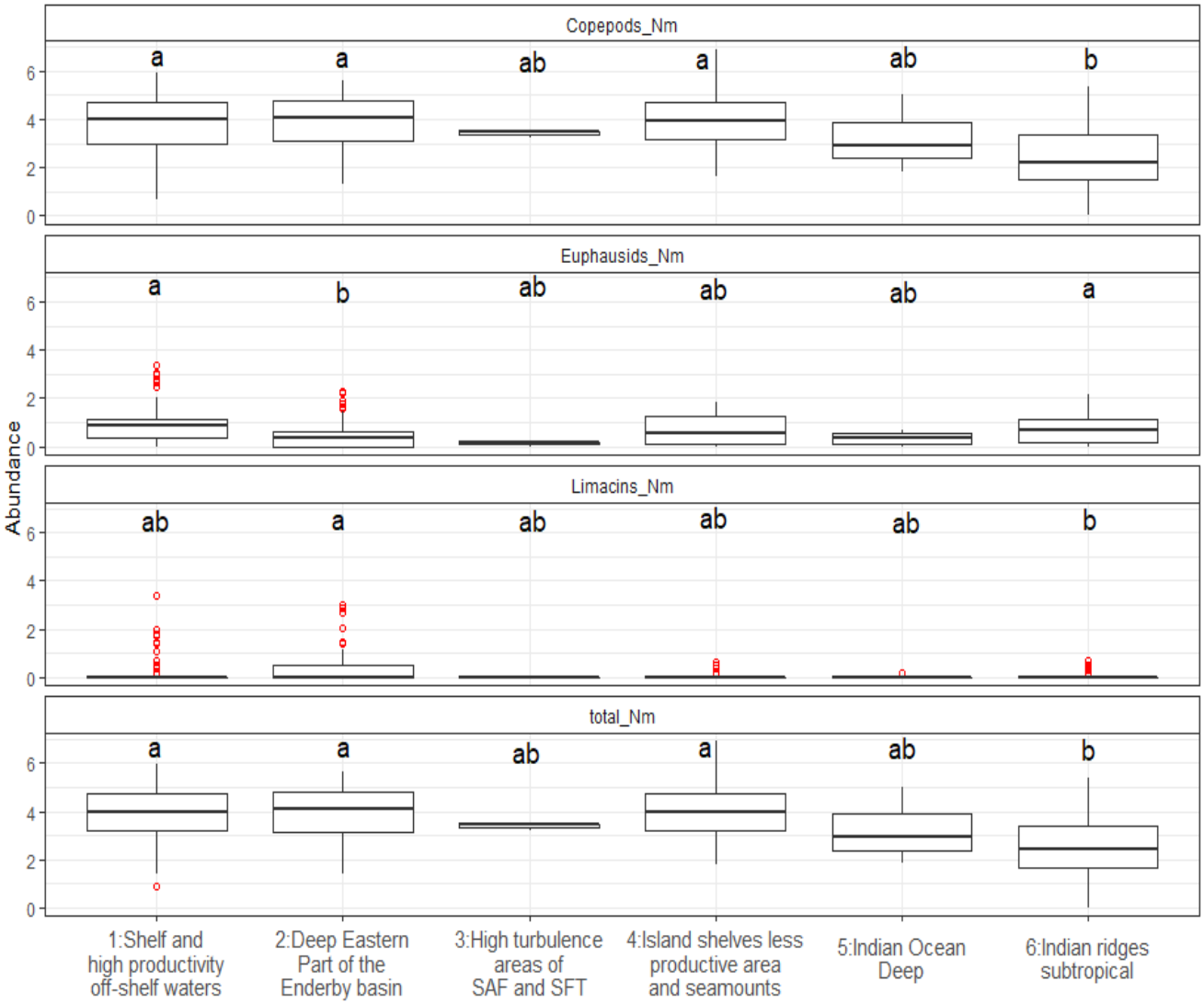

342
343

344 **Fig. 6.** Distribution of values of night abundances of copepods, euphausids and *Limacina*
345 transformed into a log (x+1) (number of individuals per nautical mile (Nm)) according to the
346 different bioregions (the sample sizes for each Bioregion: Bioregion 1: 77 samples; Bioregion
347 2: 84 samples; Bioregion 3: 3 samples; Bioregion 4: 43 samples; Bioregion 5: 11 samples;
348 Bioregion 6: 120 samples). Following the Wilcoxon post-hoc tests, the letters (a, b, c, d, e)
349 correspond to the representation of significance. If two bioregions share the same letter then
350 they are not significantly different, and, on the contrary, if two bioregions do not share the
351 same letter, then they are significantly different.

352 **3.5. Variations in zooplankton abundance with environmental parameters**

The first GLM model showed that the night abundance of copepods was significantly related to mean SST and KE. Specifically, the abundance of copepods decreased as the mean SST increase, whereas it slightly increased as the mean KE increased (Fig. 7).

The second GLM model showed that the night abundance of euphausids was significantly related to the mean Chl-*a* concentration. Specifically, the abundance of euphausids increased as the mean Chl-*a* increased (Fig. 7).

The third GLM model showed that the night abundance of *Limacina* was significantly related to mean Chl-*a* and Bat. Specifically, the abundance of *Limacina* increased as the mean Chl-*a* increased and decreased as the mean Bat increased (Fig. 7).

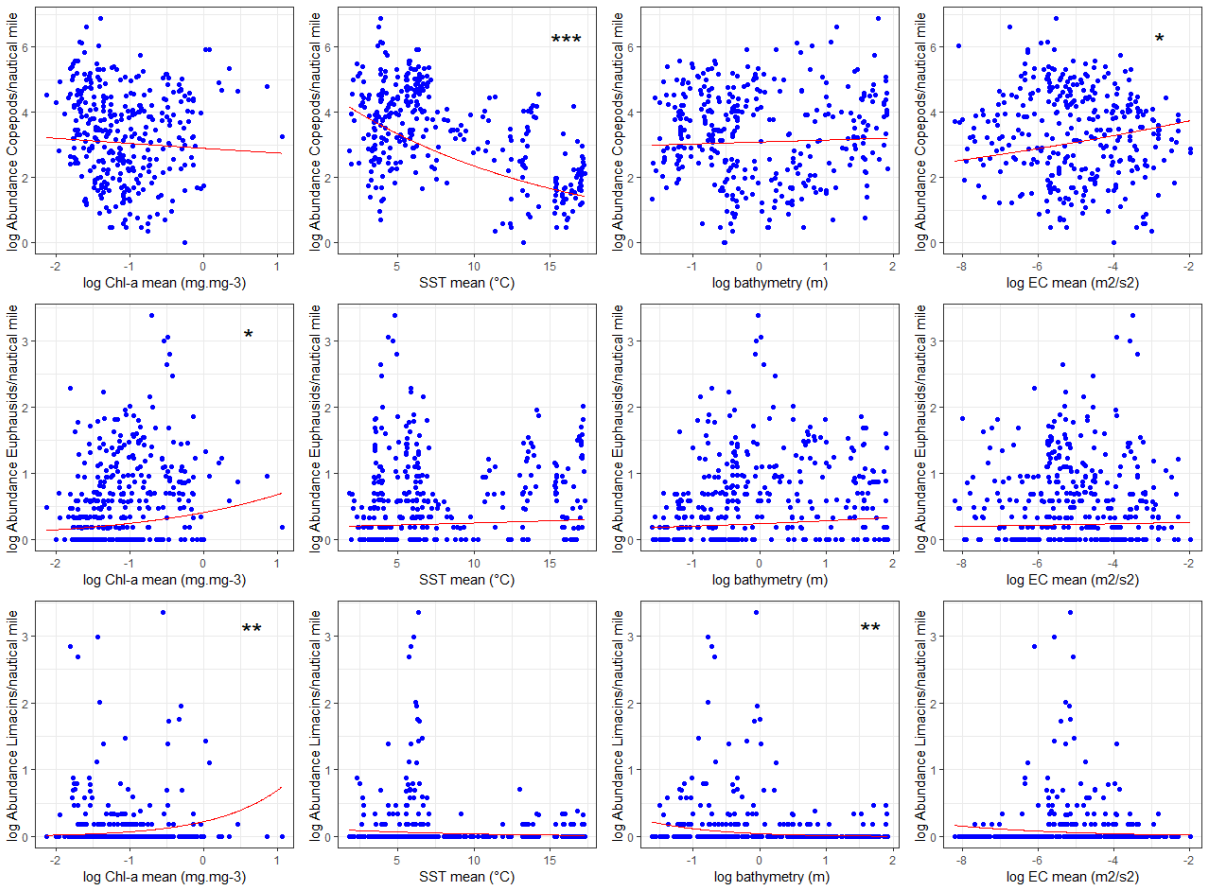

Fig. 7. Log(x+1) of night abundances of the different taxa (TOP: copepods, MIDDLE : euphausids, BOTTOM: *Limacina*, all represented as the number of individuals per nautical

366 mile) as a function of the log of Chl-a: chlorophyll-*a* concentration (mg.m-^{3}), SST: sea
367 surface temperature (° C), Bat: bathymetry (m) and the log of KE: kinetic energy (m².s-²).* =
368 p < 0.05, ** = p<0.01, *** = p<0.001 (GLM).

369

370 **4. DISCUSSION**

371 In this study, we provided a new set of epipelagic bioregions for the South Indian Ocean and
372 the Indian part of the Southern Ocean at macro- and meso-scale according to their
373 environmental characteristics. Furthermore, we highlighted how the abundance of the
374 different zooplankton taxa varied spatially with environmental conditions.

375 **4.1. Bioregionalization of the Indian part of the Southern Ocean and adjacent South**
376 **Indian Ocean**

377 The six bioregions were determined according to three physical environmental parameters
378 (sea surface temperature, kinetic energy, bathymetry) and chlorophyll-*a* concentration which
379 is considered as a proxy of the surface primary production. These bioregions provide a
380 synthetic and integrated overview of contrasting environments characterized by different
381 biophysical processes (Table 2). In accordance with previous studies by Grant et al. (2006)
382 and Raymond (2014), the six bioregions we identified follow a latitudinal pattern. However,
383 our study included the Southern part of the Indian Ocean (Bioregions 3, 5 and 6 and the
384 islands of Saint Paul and Amsterdam) in addition to the Southern Ocean (Bioregions 1, 2 and
385 4). Therefore, this study provides details about the transition between these two oceans which
386 are separated by different major fronts, mainly the Sub-Antarctic and the Subtropical Fronts.
387 The main characteristics of the six bioregions are described below.

Bioregion 1 is mainly located to the east of the Kerguelen Plateau and north of the Heard Plateau, on the central and northern part of the Crozet Plateau and in a small extent, around the St. Paul Islands and the New Amsterdam Plateau. This region corresponds to areas with high chlorophyll-*a* concentrations (Fig. 3). Indeed, the distribution of chlorophyll-*a* in the Southern Ocean is dominated by a number of recurrent blooms observed downstream of islands (Sokolov & Rintoul, 2007). These blooms are sustained by the iron enrichment of water masses from the Sub-Antarctic Islands and their plateaus (Blain et al., 2001; Sanial et al., 2014; Graham et al., 2015; d'Ovidio et al., 2015).

Bioregion 2 is located in the deep eastern part of the Enderby Basin in the Southern Ocean, south of SAF. The kinetic energy is low, as well as the sea surface temperature and chlorophyll-*a* concentration, thus representing a typical HNLC zone. South of Crozet, the PF at about 50° S has a low current velocity (Park et al., 1993; Pollard and Read, 2001; Pollard et al., 2002; Pollard et al., 2007). The low chlorophyll-*a* concentrations are a consequence of iron deficiency (Boyd et al., 2000; Boyd et al., 2007; Pollard et al., 2007; De Baar et al, 2005). Indeed, this area is very deep and remote from islands, shallow plateaus or seamounts (which are the main source of iron in the region) (e.g. Ardyna et al., 2017).

Bioregion 3 corresponds to the physically-energetic areas of the Indian Ocean characterized by high kinetic energy (Fig. 3). The ACC flows mainly to the north of the Crozet and Kerguelen plateau, the latter being a major obstacle to the eastward flow of the ACC (Roquet et al., 2009). High kinetic energies in this region indicate intense horizontal velocities generated by the ACC and the Agulhas Current. After Bioregion 1, Bioregion 3 is the area with the higher chlorophyll-*a* concentration. Indeed, the intense horizontal velocities allow the transport of nutrient from the shallow topographies around the African coasts into the open ocean for thousands of kilometers sustaining the phytoplankton productivity (e.g. Ardyna et al. 2017). In addition, this area is characterized by an intense mesoscale activity associate to meanders, eddies, filaments and fronts which may also enhance the primary

414 production (e.g. Flierl and Davies, 1993; Oschlies and Graçon, 1998; Machu and Garçon,
415 2001; Lévy, 2008).

416 Bioregion 4 is characterized by shallow to mid bathymetry and low chlorophyll-*a*
417 concentrations and is located either in the deepest parts of the island shelves, mainly in the
418 western part of these shelves, and over complex seamounts (Figs. 2 and 3). The relative low
419 chlorophyll-*a* concentration in the western part of the shelf areas (Fig. 3b) may be explained
420 by the zonal location of this bioregion relatively to the plateau. Indeed, due to the main
421 eastward circulation of the ACC, the iron enrichment of the water masses is more intense in
422 the eastern part of the shelves and offshore, generating a longitudinal chlorophyll-*a* gradient
423 upstream and downstream of the plateau (e.g Sanial et al., 2014; d'Ovidio et al., 2015). This
424 difference can be observed with contrasted chlorophyll-*a* concentrations between Bioregion 4
425 (western flank, lower chlorophyll-*a* concentration) and Bioregion 1 (eastern flank, higher
426 chlorophyll-*a* concentration). The relative shallow depth of the areas of the Bioregion 4 which
427 are located offshore from the islands is explained by the numerous seamounts included in
428 these areas. These are the large Skif bank to the south-west of Kerguelen and the Elan Bank
429 south-west of Heard at the limit of the study area (Bioregion 4b in Fig. 3). South of Crozet,
430 different seamounts of smaller size such as Ob, Lena and Marion Dufresne are located near
431 the PF (Bioregion 4e in Fig. 3). The presence of shallow seamounts may also stimulate the
432 nutrient input in the euphotic layer thus sustaining higher chlorophyll-*a* concentrations
433 compared to the surrounding water of the abyssal plain (Bioregion 2) (e.g. Pitcher et al.,
434 2008).

435 Bioregion 5 is located in the Subtropical Indian Ocean (5a) and to the north of the STF
436 (5b), two areas of abyssal plains or hills (Harris et al., 2014). They are characterized by higher
437 temperatures and represent the deepest zones of the Indian Ocean. Bioregion 5a is the
438 warmest region and Bioregion 5b is the deepest region (Fig. 3) (Harris et al., 2014). The low

chlorophyll-*a* concentrations found in Bioregion 5 are typical of the hyperoligotrophic waters of the subtropical gyres (e.g. McClain et al., 2004; Morel et al., 2010).

Bioregion 6 is characterized by a large thermal amplitude and can be considered as an Indian Subtropical region with deep bathymetry and low kinetic energy. This area also includes shallower seamounts at the mid-ocean ridges (Harris et al., 2014). This area is divided into two sub-areas by Bioregion 3. However, the main part is located to the northeast of the study area, around the St Paul and Amsterdam Islands, and includes part of the Southeast Indian Ridge. The northwestern part includes part of the Southwest Indian Ridge in Indian Ocean.

4.2. Spatial variations in zooplankton abundance

Consistent with previous CPR studies conducted in various regions of the Southern Ocean, we found that copepods account for most of the zooplankton biomass (Hunt and Hosie, 2003; Hunt and Hosie, 2006a; Hunt and Hosie, 2006b; Hosie et al., 2003; Takahashi et al., 2002; Takahashi et al., 2010; Takahashi et al., 2011). Our analyses of copepods, euphausids and *Limacina* sampled at night permitted to reveal the spatial patterns in the abundance of the different taxa across our study area encompassing the Southern Ocean and the South Indian Ocean. These spatial patterns are explained by (i) the high dependence of copepod abundance on sea surface temperature and, to a lesser extent, kinetic energy; (ii) the high dependence of euphausid abundance on chlorophyll-*a* concentration; (iii) the high dependence of *Limacina* abundance on chlorophyll-*a* concentration and shallow bathymetry.

The GLM models indicate that the copepods were most abundant in the cold waters of the Southern Ocean. Accordingly, the abundance of copepods was significantly highest in Bioregions 1, 2 and 4, which are located in the southern part of the study area and correspond to the coldest zones in the Permanent Open Ocean Zones, than in Bioregion 6. This is because temperature has major effects on the physiology of zooplankton in Antarctic and is therefore

one of the main factors defining its biogeographic distributions (Pörtner et al., 2007). Furthermore, the GLM models revealed a greater abundance of copepods in physically-energetic waters. Although copepods are quite abundant in Bioregion 3, i.e. the most physically-energetic zone of our study area located in the Subtropical and Sub-Antarctic regions, their abundance in this under-sampled bioregion does not differ significantly from the others. Further *in situ* analysis of zooplankton abundance in this high turbulent region could allow us testing this relationship within pelagic bioregions.

The GLM models also revealed that euphausids were more abundant in chlorophyll-*a* rich areas. Specifically, they were significantly less abundant in low productive open ocean waters of Bioregion 2 compared to the shelf and off-shelf high productivity areas of Bioregion 1. The higher abundance of euphausids in the Indian ridges subtropical waters of Bioregion 6 could also be related to the higher chlorophyll-*a* found there. This positive relationship between the abundance of euphausids and chlorophyll-*a* is not surprising because primary production corresponds to phytoplankton, the main food of zooplankton. This further supports previous studies showing that zooplankton biomass is globally found to be positively related to the phytoplankton biomass (Irigoien et al., 2004).

The GLM models also identify a positive relationship between *Limacina* abundance and chlorophyll-*a,* and a positive relationship of *Limacina* abundance with bathymetry. Consequently, the higher abundance of *Limacina* in Bioregion 2 could be related to the more important depths found there. Although not significantly, the shallow shelves of Bioregion 1 also display lower *Limacina* abundance. Further investigations should be done in order to confirm the relationship between *Limacina* abundance and shallow topographies, poorly covered by the existing literature.

Overall, although there are correlations between the three groups of zooplankton and environmental conditions, the different zooplankton groups do not map very well onto the bioregions. Several causes could explain this. Firstly, some key transition bioregions essential

for understanding the variability of the studied region - such as Bioregion 3, the high turbulent area between the SAF and the STF - have been under-sampled. Secondly, the coarse taxonomic resolution used in this study could have hampered the identification of clear differences between bioregions. As suggested by previous studies, and given the large temperature gradient sampled, species level data would likely better reveal differences between bioregions in our study area (e.g. Hunt et al., 2011).

4.3. Limits and perspectives

The environmental parameters used in this study come from satellite observations averaged over time and space. Due to their large spatial coverage, these data can be used to distinguish spatial environmental variations between areas in two dimensions (latitude and longitude) and to explain surface variation in zooplankton abundance. However, these measurements do not take into account how environmental conditions and zooplankton abundance vary according to the vertical dimension, i.e. the depth of the zone. The environmental properties of the water column can influence the ecology of many species along the trophic webs, including top predators (Bost et al., 2009). In addition, we did not consider all the environmental parameters that can affect the abundance of zooplankton. Future studies may consider delineating bioregions in three dimensions and integrating other potentially harmful environmental parameters for zooplankton (e.g. ocean acidification, UV or nutrient levels) to better anticipate the impact of environmental changes on zooplankton in each bioregion.

4.4. Conclusion

In this study, we first characterized bioregions based on physical parameters and chlorophyll-*a*. We then investigated the variations in zooplankton abundance across these bioregions in order to move from a bioregionalization procedure towards an ecoregionalization procedure by progressively integrating species assemblages. Initially, the temporal variations in surface

abundance are explained by nocturnal migrations, i.e. zooplankton is more abundant at night in the surface layer. The variations in zooplankton abundance are also explained spatially by environmental parameters and, to a lesser degree, by the bioregions. Future campaigns in the under-sampled transition bioregions are needed to determine whether the observed variations could be explained more consistently by the bioregionalization at the meso- and macro-scale, or whether other spatial scales should be considered for their representation.

This study complements previous ecoregionalization work (Koubbi et al., 2016a; 2016b) carried out at smaller spatial scales in the ocean zone around Kerguelen and/or Crozet on the pelagic realm, including seabirds and marine mammals. This work is therefore a further step towards the identification of coherent ecoregions. Once constructed and characterized, these ecoregions will serve as a basis for optimizing marine biodiversity conservation strategies in this part of the Southern Ocean where marine reserves around Crozet, Kerguelen and St-Paul / New Amsterdam where declared by France in 2016 (Koubbi et al., 2016a; 2016b).

An important step forward in ecoregionalization would be the integration of all species in the food web - from phytoplankton to zooplankton, fish and top predators. Indeed, as the different trophic groups do not respond in the same way to spatiotemporal variations in their environment (Koubbi et al., 2011), the way forward to an ecoregionalization of this area is to identify indicator or assemblages from distinct trophic levels. Future work should therefore investigate further regionalization of less studied mesopelagic fish. Then, it would be interesting to integrate the regionalizations of the different trophic levels in order to obtain a comprehensive regionalization.

Acknowledgements

This work was supported by IPEV, the Flotte Océanographique Française, Zone Atelier Antarctique - CNRS, the European H2020 International Cooperation project MESOPP [grant number 692173] and the TAAF (Southern Lands and Antarctic French Territories) natural reserve. It is related to the SCAR Southern Ocean CPR programme and the Global Alliance CPR Surveys We thank the IPEV teams who were in charge of logistics during the oceanographic surveys, as well as the crew members of the R/V "Marion Dufresne". We warmly thank Chloé Mignard and Baptiste Sérandour for participating in processing and identification of samples, and Patrice Pruvost for taking in charge the zooplankton sampling during the 2016 survey.

References

Ainley, D. G., Ballard, G., & Weller, J. (2010). Ross Sea bioregionalization, part I: validation of the 2007 CCAMLR bioregionalization workshop results towards including the Ross Sea in a representative network of marine protected areas in the Southern Ocean. *CAMLR reference number: CCAMLR WG-EMM-10/11*.

Ardyna, M., Claustre, H., Sallée, J. B., D'Ovidio, F., Gentili, B., Van Dijken, G., ... Arrigo, K. R. (2017). Delineating environmental control of phytoplankton biomass and phenology in the Southern Ocean. *Geophysical Research Letters*, 44(10), 5016-5024. https://doi.org/10.1002/2016GL072428

Batten, S. D., Abu-Alhaija, R., Chiba, S., Edwards, M., Graham, G., Jiyothibabu, R., ... Ostle, C. (2019). A global plankton diversity monitoring program. *Frontiers in Marine Science*, 6, 321.

Béhagle, N., Cotté, C., & Ryan, T. E. (2016). Acoustic micronektonic distribution is structured by macroscale oceanographic processes across 20-50°S latitudes in the South-Western Indian Ocean. *Deep-Sea Research Part I: Oceanographic Research Papers*, *110*, 20–32. https://doi.org/10.1016/j.dsr.2015.12.007

Biavati, G. (2014). *RAtmosphere: Standard Atmospheric profiles.* Retrieved from https://cran.r-project.org/package=RAtmosphere

Blain, S., Tréguer, P., Belviso, S., Bucciarelli, E., Denis, M., Desabre, S., … Razouls, S. (2001). A biogeochemical study of the island mass effect in the context of the iron hypothesis: Kerguelen Islands, Southern Ocean. *Deep Sea Research Part I: Oceanographic Research Papers*, *48*(1), 163–187. https://doi.org/10.1016/S0967-0637(00)00047-9

569 Blain, S., Quéguiner, B., Armand, L., Belviso, S., Bombled, B., Bopp, L., … Wagener, T.
570 (2007). Effect of natural iron fertilization on carbon sequestration in the Southern Ocean.
571 *Nature*, *446*(7139), 1070–1074. https://doi.org/10.1038/nature05700

572 Bost, C. A., Cotté, C., Bailleul, F., Cherel, Y., Charrassin, J. B., Guinet, C., … Weimerskirch,
573 H. (2009). The importance of oceanographic fronts to marine birds and mammals of the
574 southern oceans. *Journal of Marine Systems*, *78*(3), 363–376.
575 https://doi.org/10.1016/j.jmarsys.2008.11.022

576 Boyd, P. W., Watson, A. J., Law, C. S., Abraham, E. R., Trull, T., Murdoch, R., … Zeldis, J.
577 (2000). A mesoscale phytoplankton bloom in the polar Southern Ocean stimulated by
578 iron fertilization. *Nature*, *407*(6805), 695–702. https://doi.org/10.1038/35037500

579 Boyd, P. W., Jickells, T., Law, C. S., Blain, S., Boyle, E. A., Buesseler, K. O., … Watson, A.
580 J. (2007). Mesoscale Iron Enrichment Experiments 1993-2005: Synthesis and Future
581 Directions. *Science*, *315*(5812), 612–617. https://doi.org/10.1126/science.1131669

582 Boyd, P. W., & Ellwood, M. J. (2010). The biogeochemical cycle of iron in the ocean. *Nature*
583 *Geoscience*, *3*(10), 675. https://doi.org/10.1038/ngeo964

584 Broad, W. J. (1998). *The Universe Below: Discovering the Secrets of the Deep Sea*. Simon
585 and Schuster, New-York, USA.

586 Calinsky, T., & Harabasz, J. (1974). A dendrite method for cluster analysis. *Communications*
587 *in Statistics-Theory and Methods*, *3*(1), 1–27. Retrieved from www.bogucki.com.pl,

588 Constable, A. J., Melbourne-Thomas, J., Corney, S. P., Arrigo, K. R., Barbraud, C., Barnes,
589 D. K. A., … Ziegler, P. (2014). Climate change and Southern Ocean ecosystems I: How
590 changes in physical habitats directly affect marine biota. *Global Change Biology*, *20*(10),
591 3004–3025. https://doi.org/10.1111/gcb.12623

592 Cotté, C., Park, Y. H., Guinet, C., & Bost, C. A. (2007). Movements of foraging king
593 penguins through marine mesoscale eddies. *Proceedings of the Royal Society B:*
594 *Biological Sciences*, *274*(1624), 2385–2391. https://doi.org/10.1098/rspb.2007.0775

595 De Baar, H. J., De Jong, J. T., Bakker, D. C., Löscher, B. M., Veth, C., Bathmann, U., &
596 Smetacek, V. (1995). Importance of iron for plankton blooms and carbon dioxide
597 drawdown in the Southern Ocean. *Nature*, 373(6513), 412.
598 https://doi.org/10.1038/373412a0

599 De Baar, H. J. W., Boyd, P. W., Coale, K. H., Landry, M. R., Tsuda, A., Assmy, P., … Wong,
600 C. S. (2005). Synthesis of iron fertilization experiments: From the iron age in the age of
601 enlightenment. *Journal of Geophysical Research C: Oceans*, *110*(9), 1–24.
602 https://doi.org/10.1029/2004JC002601

603 De Monte, S., Cotté, C., D'Ovidio, F., Lévy, M., Le Corre, M., & Weimerskirch, H. (2012).
604 Frigatebird behaviour at the ocean-atmosphere interface: Integrating animal behaviour
605 with multi-satellite data. *Journal of the Royal Society Interface*, *9*(77), 3351–3358.
606 https://doi.org/10.1098/rsif.2012.0509

607 D'Ovidio, F., Della Penna, A., Trull, T. W., Nencioli, F., Pujol, M. I., Rio, M. H., … Blain, S.
608 (2015). The biogeochemical structuring role of horizontal stirring: Lagrangian
609 perspectives on iron delivery downstream of the Kerguelen Plateau. *Biogeosciences*,
610 *12*(19), 5567–5581. https://doi.org/10.5194/bg-12-5567-2015

611 Duhamel, G., Hulley, P. A., Causse, R., Koubbi, P., Vacchi, M., Pruvost, P., ... Dettai, A.
612 (2014). Biogeographic patterns of fish. In *Biogeographic Atlas of the Southern Ocean*,
613 418–421.

614 Flierl, G. R., & Davis, C. S. (1993). Biological effects of Gulf Stream meandering. Journal of
615 Marine Research, 51(3), 529-560. https://doi.org/10.1357/0022240933224016

616 Foster, S. D., Hill, N. A., & Lyons, M. (2017). Ecological grouping of survey sites when
617 sampling artefacts are present. *Journal of the Royal Statistical Society: Series C (Applied*
618 *Statistics)*, *66*(5), 1031–1047. https://doi.org/10.1111/rssc.12211

619 Gandhi, N., Ramesh, R., Laskar, A. H., Sheshshayee, M. S., Shetye, S., Anilkumar, N., …
620 Mohan, R. (2012). Zonal variability in primary production and nitrogen uptake rates in
621 the southwestern Indian Ocean and the Southern Ocean. *Deep-Sea Research Part I:*
622 *Oceanographic Research Papers*, *67*, 32–43. https://doi.org/10.1016/j.dsr.2012.05.003

623 Graham, R. M., De Boer, A. M., van Sebille, E., Kohfeld, K. E., & Schlosser, C. (2015).
624 Inferring source regions and supply mechanisms of iron in the Southern Ocean from
625 satellite chlorophyll data. *Deep-Sea Research Part I: Oceanographic Research Papers*,
626 *104*, 9–25. https://doi.org/10.1016/j.dsr.2015.05.007

627 Grant, S., Constable, A., Raymond, B., & Doust, S. (2006). *Bioregionalisation of the*
628 *Southern Ocean*. Hobart.

629 Gutt, J., Bertler, N., Bracegirdle, T. J., Buschmann, A., Comiso, J., Hosie, G., … Xavier, J. C.
630 (2015). The Southern Ocean ecosystem under multiple climate change stresses - an
631 integrated circumpolar assessment. *Global Change Biology*, *21*(4), 1434–1453.
632 https://doi.org/10.1111/gcb.12794

633 Handegard, N. O., Buisson, L. Du, Brehmer, P., Chalmers, S. J., De Robertis, A., Huse, G., …
634 Godø, O. R. (2013). Towards an acoustic-based coupled observation and modelling
635 system for monitoring and predicting ecosystem dynamics of the open ocean. *Fish and*
636 *Fisheries*, *14*(4), 605–615. https://doi.org/10.1111/j.1467-2979.2012.00480.x

637 Harris, P. T., Macmillan-Lawler, M., Rupp, J., & Baker, E. K. (2014). Geomorphology of the
638 oceans. *Marine Geology*, *352*, 4–24. https://doi.org/10.1016/j.margeo.2014.01.011

639 Hill, N. A., Foster, S. D., Duhamel, G., Welsford, D., Koubbi, P., & Johnson, C. R. (2017).
640 Model-based mapping of assemblages for ecology and conservation management: A case
641 study of demersal fish on the Kerguelen Plateau. *Diversity and Distributions*, *23*(10),
642 1216–1230. https://doi.org/10.1111/ddi.12613

643 Hogg, O. T., Huvenne, V. A. I., Griffiths, H. J., & Linse, K. (2018). On the ecological
644 relevance of landscape mapping and its application in the spatial planning of very large
645 marine protected areas. *Science of The Total Environment*, *626*, 384–398.
646 https://doi.org/10.1016/j.scitotenv.2018.01.009

647 Holm, S. (1979). Une simple procédure de test multiple à rejet séquentiel. *Journal scandinave*
648 *de statistiques*, *6*, 65–70. http://www.jstor.org/stable/4615733

649 Hosie, G. ., Fukuchi, M., & Kawaguchi, S. (2003). Development of the Southern Ocean
650 Continuous Plankton Recorder survey. *Progress in Oceanography*, *58*(2–4), 263–283.
651 https://doi.org/10.1016/j.pocean.2003.08.007

652 Hosie, G., Mormède, S., Kitchener, J., Takahashi, K., & Raymond, B. (2014). 10.3.Near-
653 surface zooplankton communities. In *Biogeographic Atlas of the Southern Ocean* (pp.
654 422–430).

655 Hunt, B. P., & Hosie, G. W. (2003). The Continuous Plankton Recorder in the Southern
656 Ocean: a comparative analysis of zooplankton communities sampled by the CPR and
657 vertical net hauls along 140 E. *Journal of Plankton Research*, *25*(12), 1561–1579.
658 https://doi.org/10.1093/plankt/fbg108

Hunt, B. P. V., & Hosie, G. W. (2006). The seasonal succession of zooplankton in the Southern Ocean south of Australia, part I: The seasonal ice zone. *Deep Sea Research Part I: Oceanographic Research Papers*, *53*(7), 1182–1202. https://doi.org/10.1016/j.dsr.2006.05.001

Hunt, B. P. V., & Hosie, G. W. (2006). The seasonal succession of zooplankton in the Southern Ocean south of Australia, part II: The Sub-Antarctic to Polar Frontal Zones. *Deep Sea Research Part I: Oceanographic Research Papers*, *53*(7), 1203–1223. https://doi.org/10.1016/j.dsr.2006.05.002

Hunt, B.P.V., Pakhomov, E.A., Williams, R. (2011). Comparative analysis of 1980's and 2004 macrozooplankton composition and distribution in the vicinity of Kerguelen and Heard Islands: seasonal cycles and oceanographic forcing of long-term change. *Cybium, 35*, 79-92. https://doi.org/10.26028/cybium/2011-35SP-008

Irigoien, X., Huisman, J., & Harris, R. P. (2004). Global biodiversity patterns of marine phytoplankton and zooplankton. *Nature*, 429(6994), 863-867.

IPCC, 2019. IPCC Special Report on the Ocean and Cryosphere in a Changing Climate. H.-O. Pörtner, D.C. Roberts, V. Masson-Delmotte, P. Zhai, M. Tignor, E. Poloczanska, K. Mintenbeck, A. Alegría, M. Nicolai, A. Okem, J. Petzold, B. Rama, N.M. Weyer (eds.). In press.

Koubbi, P. (1993). Influence of the frontal zones on ichthyoplankton and mesopelagic fish assemblages in the Crozet Basin (Indian sector of the Southern Ocean). *Polar Biology*, *13*(8), 557–564. https://doi.org/10.1007/BF00236398

Koubbi, P., Ozouf-Costaz, C., Goarant, A., Moteki, M., Hulley, P.-A., Causse, R., … Hosie, G. (2010). Estimating the biodiversity of the East Antarctic shelf and oceanic zone for

682 ecoregionalisation: Example of the ichthyofauna of the CEAMARC (Collaborative East
683 Antarctic Marine Census) CAML surveys. *Polar Science*, *4*(2), 115–133.
684 https://doi.org/10.1016/j.polar.2010.04.012

685 Koubbi, P., Moteki, M., Duhamel, G., Goarant, A., Hulley, P. A., O'Driscoll, R., … Hosie, G.
686 (2011). Ecoregionalization of myctophid fish in the Indian sector of the Southern Ocean:
687 Results from generalized dissimilarity models. *Deep-Sea Research Part II: Topical*
688 *Studies in Oceanography*, *58*(1–2), 170–180. https://doi.org/10.1016/j.dsr2.2010.09.007

689 Koubbi, P., Guinet, C., Alloncle, N., Ameziane, N., Azam, C. S., Baudena, A.,
690 …Weimerskirch, H. (2016). Ecoregionalisation of the Kerguelen and Crozet islands
691 oceanic zone. Part I: Introduction and Kerguelen oceanic zone. *CCAMLR Document*
692 *WG-EMM-16/43.*

693 Koubbi, P., Mignard, C., Causse, R., Da Silva, O., Baudena, A., Bost, C., … Fabri-Ruiz, S.
694 (2016). Ecoregionalisation of the Kerguelen and Crozet islands oceanic zone. Part II: The
695 Crozet oceanic zone. *CCAMLR Report,* 1-50.

696 Lê, S., Josse, J. & Husson, F. (2008). FactoMineR: An R Package for Multivariate Analysis.
697 Journal of Statistical Software. 25(1). pp. 1-18.

698 Legendre, P., & Legendre, L. (1998). *Numerical ecology*. Springer, New-York, USA.

699 Lehodey, P., Conchon, A., Senina, I., Domokos, R., Calmettes, B., Jouanno, J., ... Kloser, R.
700 (2015). Optimization of a micronekton model with acoustic data. *ICES Journal of*
701 *Marine Science*, 72(5), 1399-1412.

702 Lévy, M. (2008). The modulation of biological production by oceanic mesoscale turbulence.
703 In Transport and Mixing in Geophysical Flows (pp. 219-261). Springer, Berlin,
704 Heidelberg.

Longhurst, A. R. (2010). *Ecological geography of the sea*. Elsevier.

Machu, E., & Garçon, V. (2001). Phytoplankton seasonal distribution from SeaWiFS data in the Agulhas Current system. *Journal of marine research*, 59(5), 795-812. https://doi.org/10.1357/002224001762674944

Mackey, A. P., Atkinson, A., Hill, S. L., Ward, P., Cunningham, N. J., Johnston, N. M., & Murphy, E. J. (2012). Antarctic macrozooplankton of the southwest Atlantic sector and Bellingshausen Sea: Baseline historical distributions (Discovery Investigations, 1928–1935) related to temperature and food, with projections for subsequent ocean warming. *Deep Sea Research Part II: Topical Studies in Oceanography*, *59–60*, 130–146. https://doi.org/10.1016/j.dsr2.2011.08.011

MacQueen, J. (1967). Some methods for classification and analysis of multivariate observations. *Proceedings of the Fifth Berkeley Symposium on Mathematical Statistics and Probability*, *1*(14), 281–297. https://doi.org/10.1007/s11665-016-2173-6

Martin, J. H. (1990). Glacial-interglacial CO2 change: The iron hypothesis. *Paleoceanography*, 5(1), 1-13

McClain, C. R., Signorini, S. R., & Christian, J. R. (2004). Subtropical gyre variability observed by ocean-color satellites. *Deep Sea Research Part II: Topical Studies in Oceanography*, 51(1-3), 281-301.

Meilland, J., Fabri-Ruiz, S., Koubbi, P., Monaco, C. Lo, Cotte, C., Hosie, G. W., … Howa, H. (2016). Planktonic foraminiferal biogeography in the Indian sector of the Southern Ocean: Contribution from CPR data. *Deep-Sea Research Part I: Oceanographic Research Papers*, *110*, 75–89. https://doi.org/10.1016/j.dsr.2015.12.014

727 Morel, A., Claustre, H., & Gentili, B. (2010). The most oligotrophic subtropical zones of the
728 global ocean: similarities and differences in terms of chlorophyll and yellow substance.
729 *Biogeosciences,* 7(10), 3139-3151. https://doi.org/10.5194/bg-7-3139-2010

730 NG, A. (2012). *Clustering with the k-means algorithm. Machine Learning*.

731 Oschlies, A., & Garcon, V. (1998). Eddy-induced enhancement of primary production in a
732 model of the North Atlantic Ocean. Nature, 394(6690), 266.
733 https://doi.org/10.1038/28373

734 Orsi, A. H., Whitworth, T., & Nowlin, W. D. (1995). On the meridional extent and fronts of
735 the Antarctic Circumpolar Current. *Deep-Sea Research Part I*, *42*(5), 641–673.
736 https://doi.org/10.1016/0967-0637(95)00021-W

737 Park, Y. H., Gambéroni, L., & Charriaud, E. (1991). Frontal structure and transport of the
738 Antarctic Circumpolar Current in the south Indian Ocean sector, 40–80°E. *Marine*
739 *Chemistry*, *35*(1–4), 45–62. https://doi.org/10.1016/S0304-4203(09)90007-X

740 Park, Y. H., Gamberoni, L., & Charriaud, E. (1993). Frontal structure, water masses, and
741 circulation in the Crozet Basin. *Journal of Geophysical Research*, *98*(C7), 12361–12385.
742 https://doi.org/10.1029/93jc00938

743 Park, Y. H., Pollard, R. T., Read, J. F., & Leboucher, V. (2002). A quasi-synoptic view of the
744 frontal circulation in the Crozet Basin during the Antares-4 cruise. *Deep-Sea Research*
745 *Part II: Topical Studies in Oceanography*, *49*(9–10), 1823–1842.
746 https://doi.org/10.1016/S0967-0645(02)00014-0

747 Park, Y. H., Roquet, F., Durand, I., & Fuda, J. L. (2008). Large-scale circulation over and
748 around the Northern Kerguelen Plateau. *Deep-Sea Research Part II: Topical Studies in*
749 *Oceanography*, *55*(5–7), 566–581. https://doi.org/10.1016/j.dsr2.2007.12.030

Pitcher, T. J., Morato, T., Hart, P. J., Clark, M. R., Haggan, N., & Santos, R. S. (Eds.). (2008). *Seamounts: ecology, fisheries and conservation*. John Wiley & Sons

Pollard, R. T., & Read, J. F. (2001). Circulation pathways and transports of the Southern Ocean in the vicinity of the Southwest Indian Ridge. *Journal of Geophysical Research: Oceans*, *106*(C2), 2881–2898. https://doi.org/10.1029/2000JC900090

Pollard, R. T., Lucas, M. I., & Read, J. F. (2002). Physical controls on biogeochemical zonation in the Southern Ocean. *Deep-Sea Research Part II: Topical Studies in Oceanography*, *49*(16), 3289–3305. https://doi.org/10.1016/S0967-0645(02)00084-X

Pollard, R. T., Venables, H. J., Read, J. F., & Allen, J. T. (2007). Large-scale circulation around the Crozet Plateau controls an annual phytoplankton bloom in the Crozet Basin. *Deep-Sea Research Part II: Topical Studies in Oceanography*, *54*(18–20), 1915–1929. https://doi.org/10.1016/j.dsr2.2007.06.012

Pollard, R., Sanders, R., Lucas, M., & Statham, P. (2007). The Crozet Natural Iron Bloom and Export Experiment (CROZEX). *Deep-Sea Research Part II: Topical Studies in Oceanography*, *54*(18–20), 1905–1914. https://doi.org/10.1016/j.dsr2.2007.07.023

Pondaven, P., Fravalo, C., Ruiz-Pino, D., Tréguer, P., Quéguiner, B., & Jeandel, C. (1998). Modelling the silica pump in the Permanently Open Ocean Zone of the Southern Ocean. Journal of Marine Systems, 17(1-4), 587-619.

Pörtner, H. O., Peck, L., & Somero, G. (2007). Thermal limits and adaptation in marine Antarctic ectotherms: An integrative view. *Philosophical Transactions of the Royal Society B: Biological Sciences*, *362*(1488), 2233–2258. https://doi.org/10.1098/rstb.2006.1947

772 Post, A. L., Meijers, A. J. S., Fraser, A. D., Meiners, K. M., Ayers, J., Bindoff, N. ., …
773 Raymond, B. (2014). Environmental setting. In *Biogeographic Atlas of the Southern*
774 *Ocean* (pp. 418–421).

775 R Core Team. (2018). *R: A language and environment for statistical computing*. Retrieved
776 from https://www.r-project.org/

777 Raymond, B. (2014). Pelagic Regionalisation. In *Biogeographic Atlas of the Southern Ocean*,
778 418–421.

779 Reygondeau, G., & Huettmann, F. (2014). Past, present and future state of pelagic habitats in
780 the Antarctic Ocean. *Biogeographic Atlas of the Southern Ocean*, 397–403.

781 Ropert-Coudert, Y., Hindell, M. A., Phillips, R. A., Charrassin, J. B., Trudelle, L., &
782 Raymond, B. (2014). Biogeographic Patterns of Birds and Mammals. In *Biogeographic*
783 *Atlas of the Southern Ocean* (pp. 418–421).

784 Roquet, F., Park, Y. H., Guinet, C., Bailleul, F., & Charrassin, J. B. (2009). Observations of
785 the Fawn Trough Current over the Kerguelen Plateau from instrumented elephant seals.
786 *Journal of Marine Systems*, *78*(3), 377–393.
787 https://doi.org/10.1016/j.jmarsys.2008.11.017

788 Sanial, V., van Beek, P., Lansard, B., D'Ovidio, F., Kestenare, E., Souhaut, M., … Blain, S.
789 (2014). Study of the phytoplankton plume dynamics off the Crozet Islands (Southern
790 Ocean): A geochemical-physical coupled approach. *Journal of Geophysical Research:*
791 *Oceans*, *119*(4), 2227–2237. https://doi.org/10.1002/2013JC009305

792 Sokolov, S., & Rintoul, S. R. (2007). On the relationship between fronts of the Antarctic
793 Circumpolar Current and surface chlorophyll concentrations in the Southern Ocean.

794 *Journal of Geophysical Research: Oceans*, *112*(7), 1–17.
795 https://doi.org/10.1029/2006JC004072

796 Sokolov, S., & Rintoul, S. R. (2009). Circumpolar structure and distribution of the antarctic
797 circumpolar current fronts: 1. Mean98 circumpolar paths. *Journal of Geophysical*
798 *Research: Oceans*, *114*(11), 1–19. https://doi.org/10.1029/2008JC005108

799 Spalding, M. D., Fox, H. E., Allen, G. R., Davidson, N., Ferdaña, Z. A., Finlayson, M., …
800 Robertson, J. (2007). Marine Ecoregions of the World: A Bioregionalization of Coastal
801 and Shelf Areas. *BioScience*, *57*(7), 573–583. https://doi.org/10.1641/B570707

802 Takahashi, K. T., Kawaguchi, S., Kobayashi, M., Hosie, G. W., Fukuchi, M., & Toda, T.
803 (2002). Zooplankton distribution patterns in relation to the Antarctic Polar Front Zones
804 recorded by Continuous Plankton Recorder (CPR) during 1999/2000 Kaiyo Maru cruise.
805 *Polar Bioscience*, *15*, 97–107. https://doi.org/10.1016/j.polar.2011.04.003

806 Takahashi, K. T., Hosie, G. W., Kitchener, J. A., McLeod, D. J., Odate, T., & Fukuchi, M.
807 (2010). Comparison of zooplankton distribution patterns between four seasons in the
808 Indian Ocean sector of the Southern Ocean. *Polar Science*, *4*(2), 317–331.
809 https://doi.org/10.1016/j.polar.2010.05.002

810 Takahashi, K. T., Hosie, G. W., McLeod, D. J., & Kitchener, J. A. (2011). Surface
811 zooplankton distribution patterns during austral summer in the Indian sector of the
812 Southern Ocean, south of Australia. *Polar Science*, *5*(2), 134–145.
813 https://doi.org/10.1016/j.polar.2011.04.003

814 Turner, J., Barrand, N. E., Bracegirdle, T. J., Convey, P., Hodgson, D. A., Jarvis, M., …
815 Klepikov, A. (2014). Antarctic climate change and the environment: an update. *Polar*
816 *Record*, *50*(3), 237–259. https://doi.org/10.1017/S0032247413000296

817 Venkataramana, V., Anilkumar, N., Naik, R. K., Mishra, R. K., & Sabu, P. (2019).
818 Temperature and phytoplankton size class biomass drives the zooplankton food web
819 dynamics in the Indian Ocean sector of the Southern Ocean. *Polar Biology*, *42*(4), 823–
820 829. https://doi.org/10.1007/s00300-019-02472-w

821 **Appendix**

822 **Appendix A.** Outputs of the elbow method (A) and the method of the Calinski Harabasz
823 index (B) which were used was used to choose the optimal number of clusters and determined
824 the 6 bioregions of our study

825

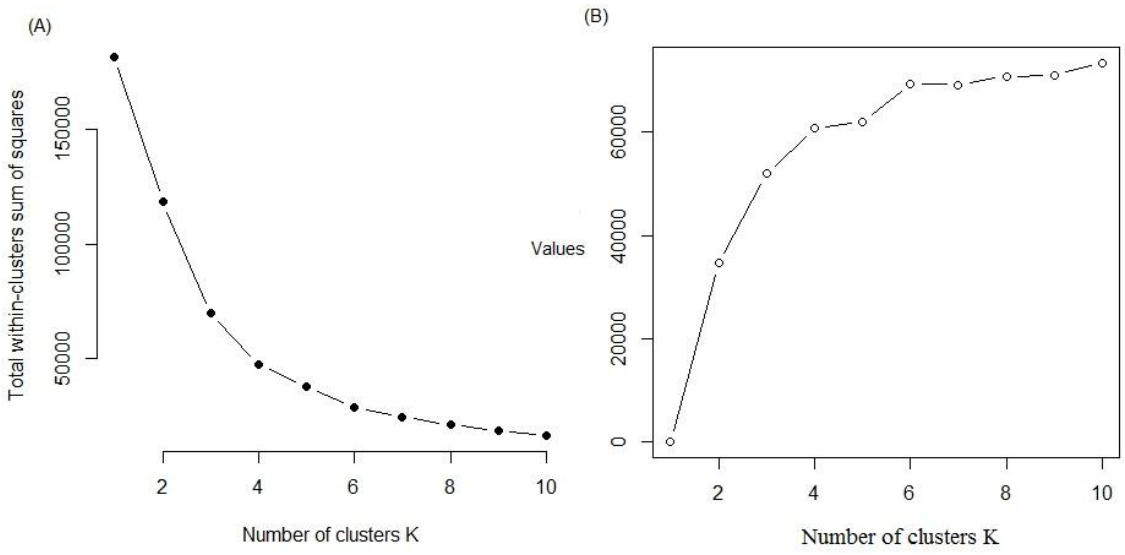

826

827